Wood Membrane Filter for Water Purification with Radial and Axial Flows

Tong Su,[a] Jianjun Xie,[a] Weiyu Chen,[a] Bo Yu,[b] Yunfeng Gu,[a] and Gensheng Wu [a,*]

Water availability is an important issue all over the world, and membrane filtration technology is one of the most effective measures for remediation. As a sustainable and renewable biomass material, natural wood has a hierarchical and three-dimensional interconnected microstructure, which provides an alternative for water filter design. Longitudinal filtration could take advantage of the micropores, while the treatment speed is severely limited. This study examined a wood filter in which muddy wastewater can be transported into the microchannels and out of the vertically stacked micropores. The filter takes full advantage of the pores present in the wood without sacrificing the speed of hydraulic flow within the main transport channels, exhibiting excellent performance for mud removal. In this manner, water flux, decolorization, and turbidity are highly dependent on the groove number, groove depth, and thickness of the filter. Due to the reorientation of the water transport pathways, the clogging of micropores could be easily alleviated, thus promoting the filter lifecycle. The design of the cross-flow wood filter can provide an available platform for various wastewater treatment cases with different impurities, displaying an application prospect in the wastewater treatment field.

DOI: 10.15376/biores.18.4.7539-7550

Keywords: Wood membrane filter; Vessels; Permeation; Water treatment; Groove design; Tilia

Contact information: a: College of Mechanical and Electronic Engineering, Nanjing Forestry University, Nanjing 210037 China; b: College of Science, Nanjing Forestry University, Nanjing 210037 China;
** Corresponding author: genshengwu@njfu.edu.cn*

INTRODUCTION

Clean water shortages affect all of humankind (Hou *et al*. 2019; Zhu *et al*. 2021a,b). In the production of potable water, membrane filtration alleviates water stress by separating particles, microorganisms, and macromolecules from sewage. Carbons, zeolites, and other conventional membrane materials have been used in filtration technology, but these materials have some deficiencies, such as high cost and poor recyclability (Das *et al*. 2014; Yang *et al*. 2018). Additionally, polymer materials from petroleum products have been utilized in water treatment, but the production and disposal of these materials generates substantial waste, which poses an environmental threat (Cai *et al*. 2022). To develop an efficient, simple, and sustainable membrane filtration technique, material innovation can play an essential role. Traditional natural biomass materials are easily accessible and cost-effective (Chen *et al*. 2022; Li *et al*. 2022), and they provide unique opportunities for developing efficient filtration technology and reducing the dependence on non-renewable materials (Huggins *et al*. 2016; Luo *et al*. 2022).

Wood is a sustainable, renewable, biodegradable, and environmentally friendly bio-composite material (Song *et al*. 2018; Chen *et al*. 2020; He *et al*. 2020). It is primarily

copolymerized with different types of cells and tissues and has a fine, multi-scale hierarchical structure (Liu *et al*. 2005; Guan *et al*. 2018). The xylem of wood is composed of abundant lumens (vessels and tracheids), fibers, and wood parenchyma lined with smaller micropores (pits, ray cells, and nanopores), naturally forming a three-dimensional (3D) interconnected porous structure (Sperry 2003; Tokareva *et al*. 2007; He *et al*. 2020). Pits on the channel walls feature excellent rejection performance due to nanoscale pores on pit membranes, which can reject particulates in the 200 nm range (Choat *et al*. 2008; Boutilier *et al*. 2014). Additionally, wooden materials resist cracking in the presence of water due to their shrinkage and swelling properties (Boutilier *et al*. 2014; Franke *et al*. 2022). Hence, natural wood has been investigated as a potential filtration material, and the 3D interconnected porous structure has inspired the design of novel water treatment devices. Sens *et al*. (2015) proposed a tubular filter and conducted the first filtration experiment along the perpendicular growth direction of wood, which was verified to be insignificant due to the lower filtration speed and higher pressure.

To date, the main challenge for wood membrane application is the fact that, based on current technology, a high filtration rate and superior water treatment cannot be realized simultaneously. To bridge this gap, this study focused on the structure design of this wood membrane. To reach a high water treatment effect, the primitive water should have a long enough pathway. However, increasing the thickness of the wood membrane to enhance the treatment effect will lead to low filtration efficiency. In this work, a two-directional-flow wood filter was proposed for solid-liquid separation by carving rectangular grooves on one side of natural basswood in the perpendicular direction of vessels. The term "two-directional-flow" refers to two perpendicular water transport pathways. Due to the 3D interconnected porous structure, the two-directional-flow wood filter has reoriented the flow path of fluid in wood, taking full advantage of the smaller pores of natural basswood without losing the speed of hydraulic flow through the main transport microchannels. As a proof of concept, the two-directional-flow wood filter showed efficient water treatment in separating mud from river water by simultaneously considering water flux, decolorization rate, and turbidity removal rate. The two-directional-flow wood filter with a 3D mesostructure provides a cost-effective platform for water treatment.

EXPERIMENTAL

Materials

The basswood (*Tilia*) was purchased from Russia with initial water content of 13% and air-dry density of 0.55 g/cm^3. Alcohol (EtOH) was purchased from Yatai Corporation of Wuxi. Ltd. The water prepared to be filtered was obtained from the Dongtan River in Nanjing Forestry University.

Preparation of the Two-directional-flow Wood Filter for Pollutants Removal

Basswood was cut along the growth direction of trees to acquire a longitudinal wood block 40 (axial) × 40 (tangential) × x (radial) mm^3 in size (x is the block depth). Rectangular grooves (30 × 2 × y mm^3, y is the groove depth) were uniformly carved on one side of wood blocks to obtain a two-directional-flow wood filter, and the schematic diagram is shown in Fig. 1.

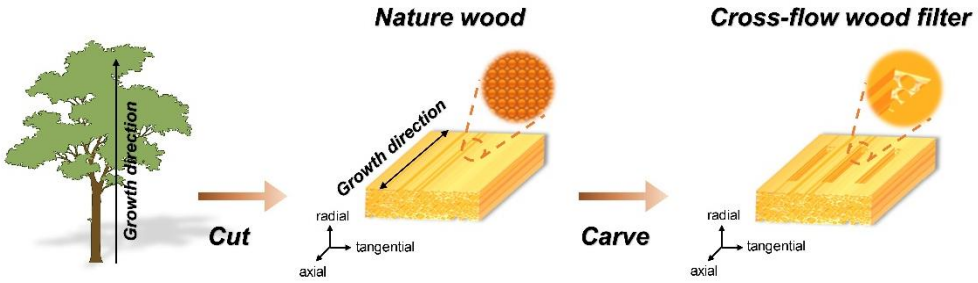

Fig. 1. Schematic illustration of the preparation of the two-directional flow wood filter

Water Treatment Measurements

The experimental wastewater filtration equipment was mainly composed of a filter and a vacuum pump used to regulate the treatment speed. The carved wood was fixed inside the filter with glass cement. A space was left on the open sides. To investigate the water treatment performance of the two-directional-flow wood filter, 20 mL of river water and 0.33 mL of mud were mixed to form an aqueous solution. The aqueous solution was then filtrated through the two-directional-flow wood filter, using vacuum filtration. The volume of solution (L) passing through the filter by unit area (m^2) and unit time (h) was measured to obtain the water flux (L/(m^2·h)) of the sample. The solution turbidity was measured by the turbidimeter (ZD-10A) and the turbidity removal rate (R_1, %) was calculated by Eq. 1,

$$R_1 = \left[\left(C_1 - C_2 \right) / C_1 \right] \times 100\% \quad (1)$$

where C_1 is the initial turbidity (NTU), and C_2 is the turbidity after filtration. Ultraviolet-visible (UV-vis) spectroscopy measurement was used to analyze the water before and after treatment in the scanning range of 250 to 400 nm on a U-T5C spectrophotometer. The solution color was determined by the top of the absorbance peak, and the decolorization rate (R_2, %) was calculated using Eq. 2,

$$R_2 = \left[\left(A_1 - A_2 \right) / A_1 \right] \times 100\% \quad (2)$$

where A_1 and A_2 are the decolorization before and after filtration, respectively. 2 mL of Alcohol was added to 20 mL of DI water, and then the wood filters were washed three times before each filtration process. The permeability (k, L/(m^2·h·bar)) was calculated using Eq. 3 (Vitas *et al*. 2019),

$$k = \frac{Q}{P} A \quad (3)$$

where Q is the measured water flux, A is the filtration area, and P is the filtration pressure.

Characterization

The morphologies of hierarchical basswood were characterized by scanning electron microscopy (SEM, Quanta 200). Ultraviolet-visible spectrophotometry (UV-vis) tests were carried out on a UV-vis spectrophotometer (U-T5C).

RESULTS AND DISCUSSION

Figure 2 shows the schematic of a two-directional-flow wood filter and an uncarved wood filter. As shown in Fig. 2(a), compared with an uncarved wood filter, grooves were

carved on one side of basswood perpendicular to the growth direction to facilitate the water entering. Water flows into the upper microchannel of the wood along the growth direction and sustains permeation through pits, ray cells, and nanopores that line the channel walls. Both sides of the two-directional-flow wood filter are open so that water can flow back into the lower microchannel and finally flow out from the bottom layer. For an uncarved wood filter, water can enter these micropores packed perpendicularly in basswood, which is subjected to high flow resistance, as shown in Fig. 2(b).

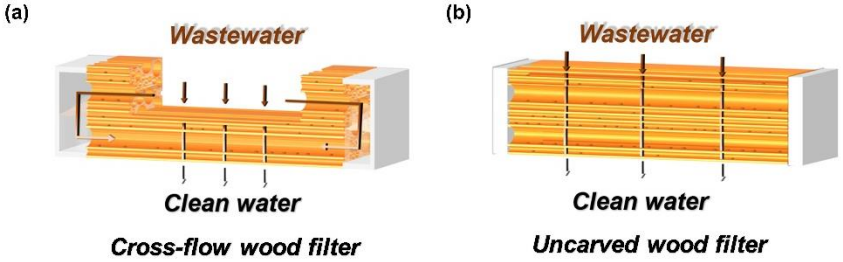

Fig. 2. Schematic design of (a) a two-directional flow wood filter and (b) an uncarved wood filter

Figure 3 shows the water treatment performance of two-directional-flow wood filters by changing groove number and groove depth. Here, water flux, decolorization rate, and turbidity removal rate were used to show the treatment efficiency. Figures 3(a)-(c) exhibit the treatment efficiency comparison for the two-directional-flow wood filter and the uncarved wood filter. Experimental results suggest that for a 5 mm-thick uncarved wood filter, a higher decolorization and turbidity rate were observed at 83.5% and 99%, respectively, and the water flux was just 1.56 L/(m^2·h). In contrast, the water flux of a 5 mm-thick two-directional-flow wood filter with 3 grooves and 2-mm depth can reach 9.12 L/(m^2·h), which is approximately 6 times that of the uncarved wood filter as shown in Fig. 3(a). Furthermore, the decolorization rate and turbidity removal rate of the two-directional-flow wood filter exhibited some loss but still were able to maintain performance of 81.2% and 97.9%, as shown in Fig. 3(b) and Fig. 3(c), respectively. The long time contact of water with inner channel walls can maintain a desirable water treatment effect. In the two-directional-flow wood filter, the water can also have adequate contact with the inner channel walls, but with much lower flow resistance.

To explore the influence of two-directional-flow design structure, an analysis of variance was used to determine the relationship between the groove number and the groove depth. As shown in Table S1(a)-(c), the effect of groove depth on water treatment performance was much greater than that of groove number, and the interaction between the two factors had no significant influence ($P>0.01$). Driven by the pressure difference of 0.2 MPa, a significant increase in water flux was realized by simultaneously increasing groove depth and number. Both the decolorization rate and the turbidity removal rate were slightly reduced, as shown in Fig. 3(d)-(f).

The promotion of water flux can be attributed to the enlarged flow area of the two-directional-flow wood filter as the number of grooves and depth are both increased. During the filtration process, the muddy wastewater was broken into microfluids and then flowed through numerous vessels and fibers inside the open sides of the filter. The microfluids permeated through the micropores into adjacent microchannels, and the solid particles were rejected in the wood. Nevertheless, the membrane formed by these micropores has been reduced into a deep groove, which is essential for excellent water treatment performance.

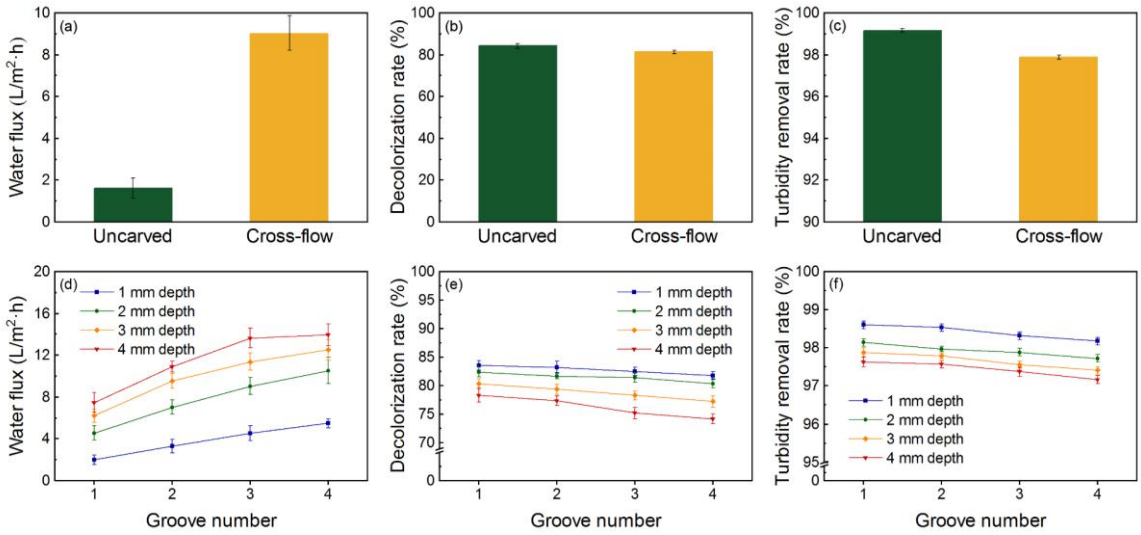

Fig. 3. Water treatment performance of an uncarved wood filter and a two-directional flow wood filter. Comparison of two different filters in terms of (a) water flux, (b) decolorization rate, and (c) turbidity removal rate. (d) The Water flux, (e) decolorization rate, and (f) turbidity removal rate at different groove numbers and depths

Natural wood has a hierarchical structure with diverse distribution and connectivity of pores in different directions (Yin *et al*. 2015; Shen *et al*. 2021; Ru *et al*. 2023), which provides more contact for water filtration. The water treatment performance of the two-directional-flow wood filter with different thickness was compared. The water before and after treatment was analyzed quantitatively by UV. Figure 4a illustrates that the intensity of the characteristic absorbance band at 295 nm declined dramatically after filtration, and the decline in absorbance tended to be stable as the thickness exceeded 8 mm. As shown in Fig. 4b, it was conducive to the water treatment effect by increasing the thickness of the two-directional-flow wood filter, while the water flux was gradually decreased. A 10 mm-thick two-directional-flow wood filter was about only 3.44 L/(m^2·h). As the filter thickness reduced to 3 mm, the decolorization rate and turbidity removal rate dropped sharply, but the water flux increased to 14.5 L/(m^2·h).

The muddy wastewater turned clean after passing through an 8 mm-thick two-directional-flow wood filter with a decolorization rate of 92%, a turbidity removal efficiency of 99%, and a water flux of 6.75 L/(m^2·h), which represents one of the best water treatment performances of the two-directional-flow wood filter among all samples.

To investigate the influence of the mud mixing ratio on the treatment capacity, the water treatment efficiency was evaluated over a mixing ratio ranging from 1:100 to 1:20. As shown in Fig. 5a, even at a relatively higher mixing ratio (1:20), a high decolorization rate and turbidity removal efficiency could still be achieved by this two-directional-flow wood filter, which can reach around 92% and 98%, respectively. The permeability of the filter was tested as a function of water flux and pressure difference, which were controlled by a vacuum pump, and the results are plotted in Fig. 5b. During the vacuum filtration process, the filter provided better permeability without sacrificing water treatment effect with a pressure difference of 0.2 MPa between the two sides. Based on this material platform (*i.e.*, an 8 mm-thick two-directional-flow wood filter with 3 grooves and 2 mm depth), other pollutants can be removed easily from water. Here, two different kinds of wastewater contaminated with red ink and turbid liquid were treated. As shown in Fig. S1a,

the contents of two kinds of pollutants were dramatically reduced after the wastewater passed through the same two-directional-flow wood filter, which is essential for the natural wood as a potential filtration device.

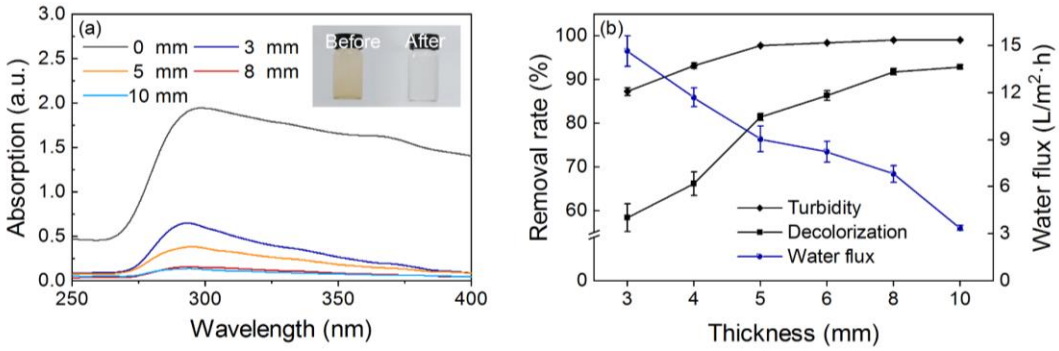

Fig. 4. (a) Ultraviolet-visible absorption spectroscopy of the filtrate, (b) calculated water flux, decolorization rate, and turbidity removal rate with respect to the filter thickness

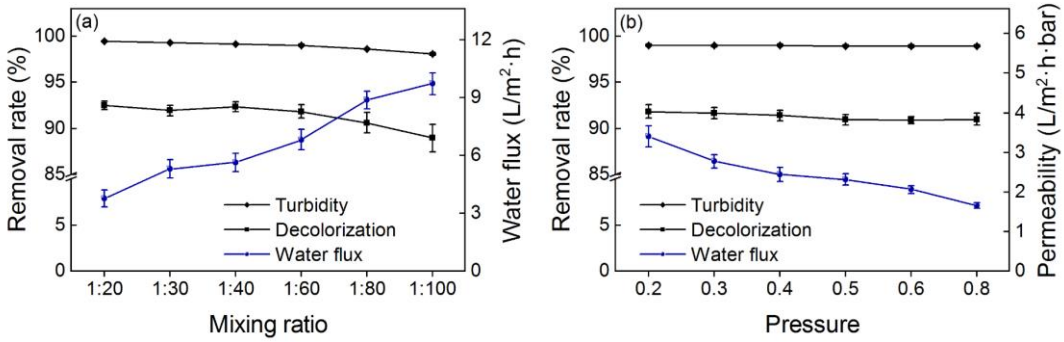

Fig. 5. Water treatment performance with respect to (a) mud mixing ratio and (b) filtration pressure

The promising water treatment capacity of the two-directional-flow wood filter originates from the fluid flow as regulated by the exposed microchannels. Figure 6a shows that basswood is densely packed with abundant fibers and vessels. Large-diameter vessels are connected along the growth direction by perforation plates, providing an elongated pathway as the main channel for water transport (He *et al*. 2020). In this case, the fast hydraulic flow of fluid in vessels might be beneficial to reduce the detachment of particulates adhered to the surface of vessel walls, ultimately extending the longevity of the wood filter (Sens *et al*. 2015). As shown in Fig. 6b, the SEM image shows numerous pits on the vessel walls. The rejection functionality of the xylem is largely determined by the bordered pits and other nanopores that connect adjacent vessels and fibers. Different layers of pit membranes are positioned in series rather than in parallel, and a larger wood filter thickness potentially further expands the total membrane area of pits (Boutilier *et al*. 2014). The microstructure of the filter was further characterized after filtration. Figure 6c shows the retained impurities on the inner surface of vessels. With the extension of filtration time, the hydraulic resistance of these micropores increases gradually due to decreased porosity caused by fouling, which still deserves further study for practical applications.

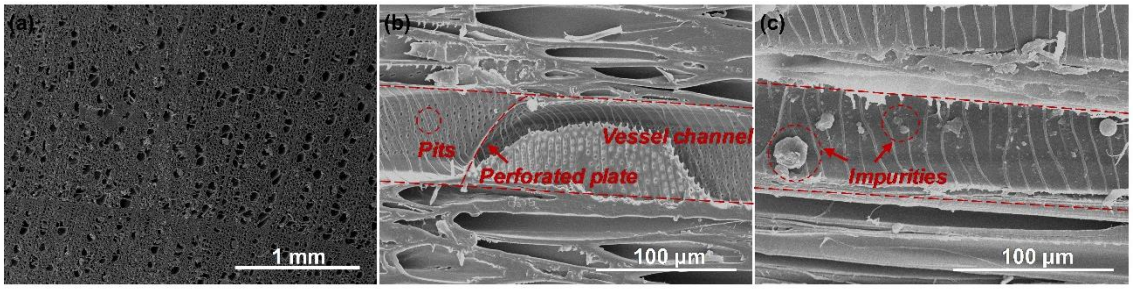

Fig. 6. (a) SEM image of the wood transverse section. Magnified SEM image of the detailed microstructure of a single vessel channel (b) before and (c) after filtration

The microscopic flow distribution characteristics and the movement of particles driven by hydrostatic fluid in the wood microchannels were investigated. For basswood, the vessel determines water flow into the main channels, and cross-channel transport is mainly dominated by pits (Chen *et al*. 2017). To provide an illustration for the enhanced filtration by two-directional-flow structure, the water transport within a single vessel was investigated. A three-dimensional model of a single microchannel was established based on SEM images as well as the previously reported geometries of vessels in basswood (Xu *et al*. 2020). As shown in Fig. 7a, a section of extended smooth area was added at the two ends of the channel in order to reduce the influence of inlet and outlet flow rates. By changing the diameter, this particular channel model can be regarded as a unit that repeats in the microstructure of the wood filter as conducted in a computational fluid dynamics (CFD) simulation. Figure 7b exhibits that in the control model, water flows into the top half cylindrical surface of the channel and flows out of the bottom half cylindrical surface and two side channels. In contrast, the flow can occur through the open sides of the two-directional-flow wood filter, and the left outlet of the two-directional-flow model was altered to an entry while leaving the other arguments intact, as seen in Fig. 7c.

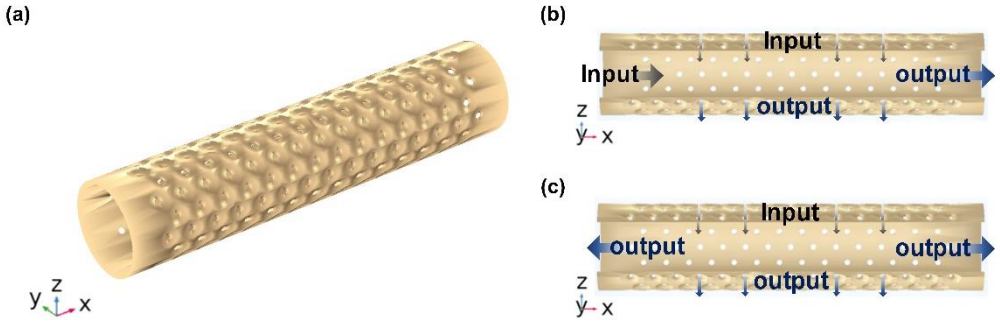

Fig. 7. (a) A 3D model of a single microchannel. Schematic of water flow (b) in control and (d) in cross-directional flow.

Considering that the microchannel model would continue to be submerged in the liquid, the hydrostatic pressure drop between the inlet and outlet was calculated at 759.75 pa (101.3 kPa/0.8 cm × 60 μm) (He *et al*. 2020). It is assumed that the microfluidic water transport in the wood microporous structure is steady, incompressible, and governed laminar (Xu and Zhang 2020). In this case, the fluid flow can be described by Navier-Stokes Eq. 4,

$$\begin{cases} \rho u \nabla u = \nabla \left\{ -pI + \eta \left[\nabla u + (\nabla u)^T \right] \right\} + F \\ \nabla u = 0 \end{cases} \quad (4)$$

where u is the flow velocity, I is the identity tensor, ρ is fluid density, η is the dynamic viscosity, p is the pressure, respectively.

The flow contours of velocity vector distributions at the steady state in different models are shown in Fig. 8a and Fig. S2a, with the color indicating the velocity magnitude. These flow contours demonstrate that the velocity in the control model is lower than that in the two-directional-flow model. Additionally, the flow is distributed on opposite sides of the main channel, which considerably disturbs the unidirectional nature of the fluid flow and aggravates its energy loss. For the two-directional-flow, the velocity in the cross-section of the channel is trapeziform and totally laminar, with a lower velocity on the narrow side and a higher velocity in the center. The flow trajectories were studied for fluid tracer particles in four separate channels, including control and two-directional-flow with two different diameters. As shown in Figure 8b and Figure S2b, numerous particles were captured in the bottom half cylindrical pit surface under pressure in the control channel. By contrast, the two-directional-flow is beneficial to filtering since the higher velocity accumulates particles and thus efficiently separates out water from the outlet pits.

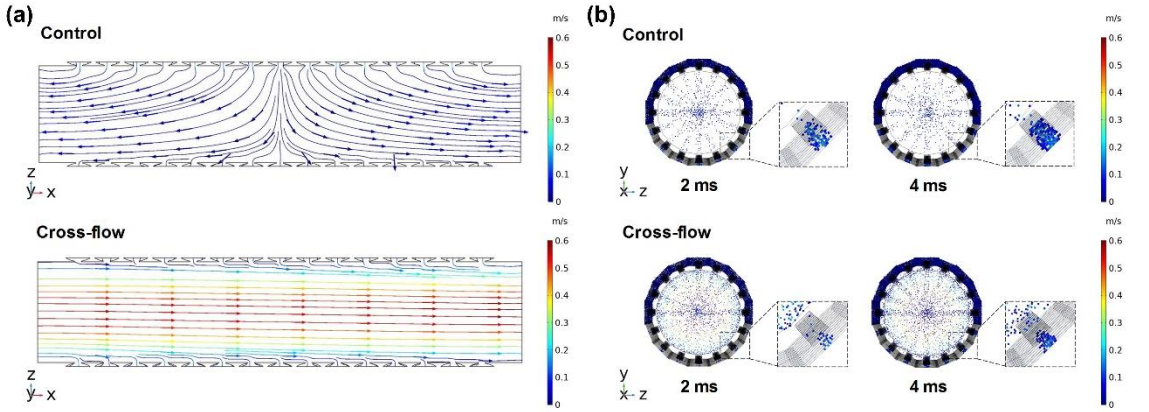

Fig. 8. Schematic of (a) fluid flow along the channel (60 μm in diameter) in cross section and (b) distribution of particles

The above results were further demonstrated by the particle amount in Fig. 9a. Along with the continuous release of particles, it is noted that the speed in the control filter was three times quicker than that in two-directional-flow design, while the diameter had a negligible impact, comparatively. Note that the pits connecting the adjacent longitudinal channels play a vital role in water transportation (Chen *et al*. 2017). As indicated in Fig. 9b, the flow through the bottom half cylindrical pit surface is gradually increased with the increasing of pit amount. The two-directional-flow design triggers an effect of increased water flux and an abated surface area for particle exposure (or lessened pit clogging). These factors ultimately ensure that prolonged utilization occurs throughout the entire wood block owing to the microstructure of the natural wood.

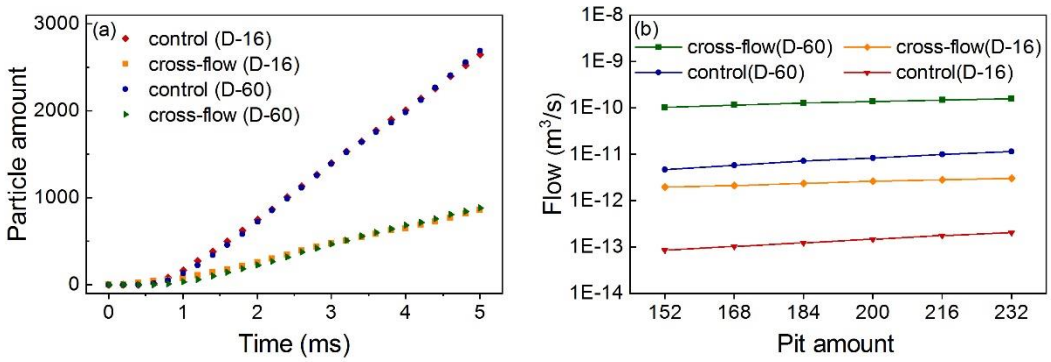

Fig. 9. (a) Relationship between time and particle amount through the bottom half cylindrical pit surface. (b) Relationship between pit amount and flow through the bottom half cylindrical pit surface

CONCLUSIONS

1. A two-directional-flow wood filter reorients the flow path of fluid in wood microchannels for high water treatment speed. Due to the open-sided design with a large quantity of exposed incisions, the two-directional-flow wood filter provided abundant fluid transfer channels and augmented the inlet area for water transportation. Additionally, the series arrangement of pits, ray cells, and nanopores on the cell walls exhibited suitable rejection ability.
2. Experimental results showed that the decolorization efficiency and turbidity removal efficiency of an 8 mm-thick two-directional-flow wood filter with 3 grooves and 2 mm depth can reach around 92% and 98% at a water flux up to 6.75 L/(m^2·h), respectively. It is worth noting that the clogging issue of micropores could be easily alleviated by the unidirectional nature of water transport, which enhances the utilization of filters.
3. The two-directional-flow wood filter with an interconnected hierarchical 3D network consisting of partially aligned microchannels and micropores could be extended to various water treatment processes with diverse impurities. This platform based on renewable materials offers enhanced water treatment performance with low cost and power consumption, benefiting the environment.

ACKNOWLEDGMENTS

This work was supported by the National Natural Science Foundation of China (51905276) and Natural Science Foundation of Jiangsu Province (BK20200787).

REFERENCES CITED

Boutilier, M., Lee, J., Chambers, V., Venkatesh, V., and Karnik, R. (2014). "Water Filtration using plant xylem," *Plos One* 9(2), article ID e89934. DOI: 10.1371/journal.pone.0089934

Cai, Z., Liu, Y., Tao, Y., and Zhu, J. (2022). "Recent advances in monomer design for recyclable polymers," *Acta Chimica Sinica* 80(8), 1165-1182. DOI:

10.6023/A22050235

Chen, C., Kuang, Y., Zhu, S., Burgert, I., Kepling, T., Gong, A., Li, T., Berglund, L., Eichhorn, S. J., and Hu, L. (2020). "Structure-property-function relationships of natural and engineered wood," *Nature Reviews Materials* 5(9), 642-666. DOI: 10.1038/s41578-020-0195-z

Chen, F., Gong, A. S., Zhu, M., Chen, G. Lacey, S. D., Jiang, F., Li, Y., Wang, Y., Dai, J., Yao Y., Song J., Liu, B., Fu, K., Das, S., and Hu, L. (2017). "Mesoporous, three-dimensional wood membrane decorated with nanoparticles for highly efficient water treatment," *ACS Nano* 11(4), 4275-4282. DOI: 10.1021/acsnano.7b01350

Chen, K., Ng, K. H., Cheng, C. K., Cheng, Y. W., Chong, C. C., Vo D. V. N., Witoon, T., and Ismail, M. H. (2022). "Biomass-derived carbon-based and silica-based materials for catalytic and adsorptive applications – An update since 2010," *Chemosphere* 287(2), article ID 132222. DOI: 10.1016/j.chemosphere.2021.132222

Choat, B., Cobb, A. R., and Jansen, S. (2008). "Structure and function of bordered pits: new discoveries and impacts on whole-plant hydraulic function," *New Phytologist* 177(3), 608-626. DOI: 10.1111/j.1469-8137.2007.02317.x

Das, R., Ali, M. E., Abd Hamid, S. B., Ramakrishna, S., and Chowdhury, Z. Z. (2014). "Carbon nanotube membranes for water purification: A bright future in water desalination," *Desalination* 336, 97-497. DOI: 10.1016/j.desal.2013.12.026

Franke, B., Franke, S., and Schiere, M. J. (2022). "Climate impact on reinforcements in wooden members-effective hygro-expansion coefficients," *Wood Material Science & Engineering* 17(4), 299-308. DOI: 10.1080/17480272.2022.2086821

Guan, H., Cheng Z., and Wang X. (2018). "Highly compressible wood sponges with a spring-like lamellar structure as effective and reusable oil absorbents," *ACS Nano* 12(10), 10365-10373. DOI: 10.1021/acsnano.8b05763

He, S., Chen, C., Chen, G., Chen, F., Dai, J., Song, J., Jiang, F., Jia, C., Xie, H., Yao, Y., Hitz, E., Chen, G., Mi, R., Jiao, M., Das, S., and Hu, L. (2020). "High-performance, scalable wood-based filtration device with a reversed-tree design," *Chemistry of Materials* 32(5), 1887-1895. DOI: 10.1021/acs.chemmater.9b04516

He, S., Chen, C., Li, T., Song, J., Zhao, X., Kuang, Y., Liu, Y., Pei, Y., Hitz, E., Kong, W., Gan, W., Yang, B., Yang, R., and Hu, L. (2020). "An energy-efficient, wood-derived structural material enabled by pore structure engineering towards building efficiency," *Small Methods* 4(1), article ID 1900747. DOI: 10.1002/smtd.201900747

Hou, D., Li, T., Chen, X., He, S., Dai, J., Mofid, S. A., Hou, D., Iddya, A., Jassby, D., Yang, R., Hu, L., and Ren, Z. (2019). "Hydrophobic nanostructured wood membrane for thermally efficient distillation," *Science Advances* 5(8), article ID eaaw3203. DOI: 10.1126/sciadv.aaw3203

Huggins, T. M., Haeger, A., Biffinger, J. C., and Ren, Z. J. (2016). "Granular biochar compared with activated carbon for wastewater treatment and resource recovery," *Water Research* 94, 225-232. DOI: 10.1016/j.watres.2016.02.059

Li, T., Zhi, D. D., Guo, Z. H., Li, J. Z., Chen, Y., and Meng, F. B. (2022). "3D porous biomass-derived carbon materials: biomass sources, controllable transformation and microwave absorption application," *Green Chemistry* 24(2), 647-674. DOI: 10.1039/d1gc02566j

Liu, Z. T., Fan, T. X., Zhang, W., and Zhang, D. (2005). "The synthesis of hierarchical porous iron oxide with wood templates," *Microporous and Mesoporous Materials* 85(1-2), 82-88. DOI: 10.1016/j.micromeso.2005.06.021

Luo, X., Lu, R., Si, X., Jiang, H., Shi, Q., Ma, H., Zhang, C., Xu, J., and Lu, F. (2022).

"Sustainable synthesis of high-density fuel via catalytic cascade cycloaddition reaction," *Journal of Energy Chemistry* 69, 231-236. DOI: 10.1016/j.jechem.2022.01.029

Ru, Y., Hu, C., Chen, X., Yang, F., Zhang, C., Li, J., and Fang, S. (2023). "Droplet penetration model based on canopy porosity for spraying applications," *Agriculture-Basel* 13(2), article ID 339. DOI: 10.3390/agriculture13020339

Sens, M. L., Emmendoerfer, M. L., and Muller L. C. (2015). "Water filtration through wood with helical cross-flow," *Desalination and Water Treatment* 53(1), 15-26. DOI: 10.1080/19443994.2013.837010

Shen, X., Jiag, P., Guo, D., Li, G., Chu, F., and Yang, S. (2021). "Effect of furfurylation on hierarchical porous structure of poplar wood," *Polymers* 13(1), article ID 32. DOI: 10.3390/polym13010032

Song, J., Chen C., Zhu S., Zhu M., Dai J., Ray U., Li Y., Kuang Y., Li Y., and Quispe N. (2018). "Processing bulk natural wood into a high-performance structural material," *Nature* 554(7691), 224-228. DOI: 10.1038/nature25476

Sperry, J. S. (2003). "Evolution of water transport and xylem structure," *International Journal of Plant Sciences* 164(3), 115-127. DOI: 10.1021/acsnano.8b05763

Tokareva, E. N., Pranovich, A.V., Fardim, P., Danie, G., and Holmbom, B. (2007). "Analysis of wood tissues by time-of-flight secondary ion mass spectrometry," *Holzforschung* 61(6), 647-655. DOI: 10.1515/HF.2007.119

Vitas, S., Beckmann, P., Skibinski, B., Goldhahn, C., Muff, L. F., and Cabane, E. (2019). "Rejection of micron-sized particles using beech wood xylem," *Environmental Science-Water Research & Technology* 5(3), 608-626. DOI: 10.1039/c8ew00774h

Xu, T., and Zhang, L. (2020). "Analysis of water transport inside a plant xylem vessel with pitted thickening," *Fluid Dynamics & Materials Processing* 16(3), 525-536. DOI: 10.32604/fdmp.2020.09618

Xu, T., Zhang, L., and Li, Z. (2020). "Computational fluid dynamics model and flow resistance characteristics of *Jatropha curcas* L xylem vessel," *Scientific Reports* 10(1), article ID 14728. DOI: 10.1038/s41598-020-71576-9

Yang, Z., Ma, X. H., and Tang, C. Y. Y. (2018). "Recent development of novel membranes for desalination," *Desalination* 434, 37-59. DOI: 10.1016/j.desal.2017.11.046

Yin, J., Song, K., Liu, Y., Zhao, G., and Yin, Y. (2015). "Comparison of changes in micropores and mesopores in the wood cell walls of sapwood and heartwood," *Wood Science and Technology* 49(5), 987-1001. DOI: 10.1007/s00226-015-0741-9

Zhu, H., Cai, S., Zhou, J., Li, S., Wang, D., Zhu, J., Wu, Y., Huang, Y., Yuan, S., Jing, S., and Xia, F. (2021a). "Integration of water collection and purification on cactus- and beetle-inspired eco-friendly superwettable materials," *Water Research* 206, article ID 117759. DOI: 10.1016/j.watres.2021.117759

Zhu, X., Hu, J., Liu, G., Xu, D., Wei, Y., Liu. D, Chang. S., Li, X., and Liu, Y. (2021b). "Unique 3D interpenetrating capillary network of wood veneer for highly efficient cross flow filtration," *Journal of Materials Science* 56(4), 3155-3167. DOI: 10.1007/s10853-020-05478-6

Article submitted: July 12, 2023; Peer review completed: August 19, 2023; Revised version received and accepted: August 22, 2023; Published: September 19, 2023.
DOI: 10.15376/biores.18.4.7539-7550

APPENDIX

Table S1a. Two-way Analysis of Variance of Decolorization Efficiency

Factor	Square Sum	Freedom	Mean Square	F-value	Significance
A	0.005	3	0.00178	22.779	P<0.01
B	0.030	3	0.010	128.434	P<0.01
A×B	0.00089	9	9.9e-5	1.265	P>0.01
Error	0.0025	32			

Table S1b. Two-way Analysis of Variance of Turbidity Removal Efficiency

Factor	Square Sum	Freedom	Mean Square	F-value	Significance
A	1.4e-4	3	4.7e-5	46.647	P<0.01
B	6.3e-4	3	2.1e-4	209.291	P<0.01
A×B	3.4e-6	9	3.7e-7	0.374	P>0.01
Error	3.2e-5	32			

Table S1c. Two-way Analysis of Variance of Water Flux

Factor	Square Sum	Freedom	Mean Square	F-value	Significance
A	216.55	3	72.183	112.989	P<0.01
B	394.946	3	131.649	206.070	P<0.01
A×B	14.013	9	1.557	2.437	P>0.01
Error	20.443	32			

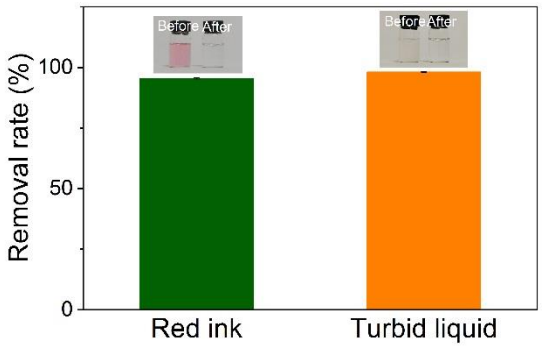

Fig. S1. (a) The treatment efficiency of the cross- flow filter for red ink and turbid liquid.

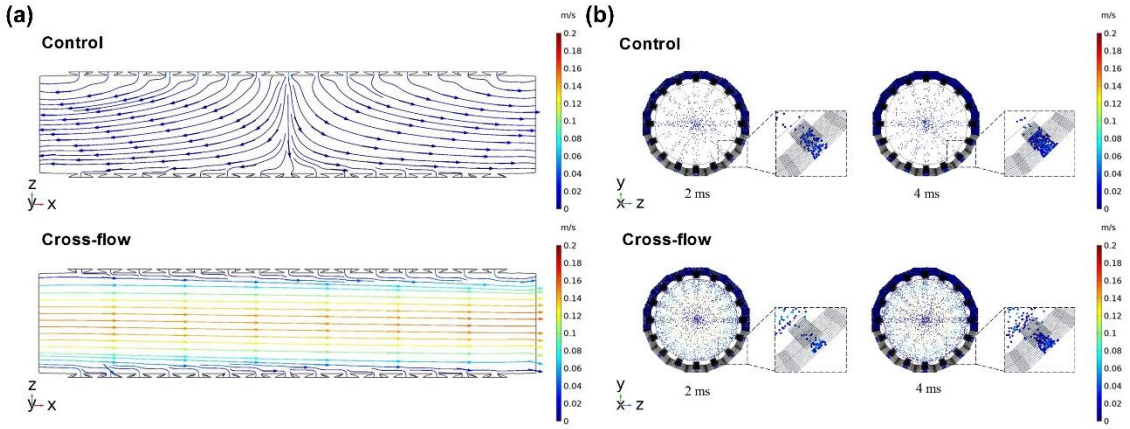

Fig. S2. Schematic of (a) fluid flow along the channel (16 μm in diameter) in cross section and (b) distribution of particles.